

Studying the nonlinear behavior of the functionally graded annular plates with piezoelectric layers as a sensor and actuator under normal pressure

M. Arefi^a and G.H. Rahimi*

*Department of Mechanical Engineering, Tarbiat Modares University, Tehran, Iran, 14115-143
(Received November 30, 2011, Revised January 7, 2012, Accepted January 18, 2012)*

Abstract. The present paper deals with the nonlinear analysis of the functionally graded piezoelectric (FGP) annular plate with two smart layers as sensor and actuator. The normal pressure is applied on the plate. The geometric nonlinearity is considered in the strain-displacement equations based on Von-Karman assumption. The problem is symmetric due to symmetric loading, boundary conditions and material properties. The radial and transverse displacements are supposed as two dominant components of displacement. The constitutive equations are derived for two sections of the plate, individually. Total energy of the system is evaluated for elastic solid and piezoelectric sections in terms of two components of displacement and electric potential. The response of the system can be obtained using minimization of the energy of system with respect to amplitude of displacements and electric potential. The distribution of all material properties is considered as power function along the thickness direction. Displacement-load and electric potential-load curves verify the nonlinearity nature of the problem. The response of the linear analysis is investigated and compared with those results obtained using the nonlinear analysis. This comparison justifies the necessity of a nonlinear analysis. The distribution of the displacements and electric potential in terms of non homogenous index indicates that these curves converge for small value of piezoelectric thickness with respect to elastic solid thickness.

Keywords: piezoelectric; nonlinear; annular plate; energy; functionally graded piezoelectric; sensor; actuator.

1. Introduction

Smart materials have been discovered about 230 years ago by Pierre and Jacques Curie in Paris. Quartz as a first piezoelectric material has been introduced. With applying an arbitrary electric potential to a piezoelectric material such as Quartz, one can find deformation in the structure. This relation and converse relation have been introduced as piezoelectric and converse piezoelectric effects, respectively. Piezoelectric structures are very applicable in the industrial systems such as measurement instruments. For example, these structures can be used as actuator or sensor. Plates, disks and cylinders are three famous structures that can be used as sensor or actuator in electromechanical systems. For these reasons, it is appropriate to investigate the relation between the applied loads, electric potential and displacement in a piezoelectric structure such as annular disk. To control the distribution of the displacement or electric potential in a piezoelectric structure, functionally graded piezoelectric material

*Corresponding author, Professor, E-mail: rahimi_gh@modares.ac.ir

^aarefi63@gmail.com

(FGPM) can be used. The properties of this material vary continuously along the coordinate system. For the structures those are applicable in the environment such as nuclear reactors and chemical laboratory, it is inevitable to use functionally graded materials (FGM's). FGM's are made of a mixture with arbitrary composition of two different materials, and volume fraction of each material changes continuously and gradually at the entire volume of the structure. Ceramic and metal are the examples of these different materials. Ceramics can bear the serious physical condition such as high temperature gradient.

Woo and Meguid (2001) studied the nonlinear analysis of the functionally graded plates and shallow shells. They proposed an analytical solution for the coupled large deflection of functionally graded (FG) plates and shallow shells. Von-Karman theory was employed for large deflection analysis. A piezoceramic hollow sphere was analytically studied based on the 3D equations of piezoelectricity by Chen *et al.* (2002). Analysis of a piezoelectric cantilever beam with functionally graded properties was presented using the Airy stress function method by Shi *et al.* (2004). Exact solutions of a rectangular laminate with piezoelectric layers of exponentially graded material properties along thickness direction and under simply supported along two opposite edges, was derived by Lu *et al.* (2005). Analytical solution of a functionally graded piezo elastic hollow cylinder was presented by Chen and Shi (2005). GhannadPour and Alinia (2006, 2009) investigated the large deflection analysis of a rectangular FG plate. Von-Karman theory was employed for the large deflection and solution was obtained using minimization of the total potential energy. Hui-Shen Shen (2007) considered the nonlinear response of FG plate due to heat conduction. It was assumed that the plate to be shear deformable. Higher order shear deformation theory was employed for analysis of the problem. Electromagnetoelastic behaviors of FGP solid cylinder and sphere are researched by Dai *et al.* (2007). They indicated that the proper mechanical and electrical loads to the FGP solid structures can control the distributions of stresses, electric potential and perturbation of magnetic field vector. Exact solution of FGP cylindrical shell under cylindrical bending was carried out by Chih and Yun-Sing (2007). Transient piezothermoelastic analysis for a hollow sphere made of functionally graded piezoelectric material was studied by Ootao and Tanigawa (2007). Allahverdizadeh *et al.* (2008) investigated the nonlinear behavior of thin circular FG plates. The analysis was assumed to be axisymmetric and solution was derived based on a semi-analytical approach. Ebrahimi and Rastgo (2008) investigated the free vibration analysis of smart circular thin FG plate using classical plate theory. The power function was used for distribution of the material properties along the thickness direction. Plate was composed of a FG layer with two FGP layers at top and bottom. The obtained results were verified by those obtained results from three dimensional finite element analyses. Malekzadeh and Vosoughi (2009) investigated the large amplitude vibration of composite beams on the nonlinear elastic foundation. The foundation was supposed that has cubic nonlinearity with shearing layer. Soufyane (2009) investigated the stability of the linearized non uniform timoshenko beam. Sarfaraz Khabbaz *et al.* (2009) investigated the nonlinear analysis of FG plates under pressure based on the higher-order shear deformation theory. They used the first and higher order shear deformation theory to investigate the large deflection of FG plate. The effect of thickness and non homogenous index was investigated on the distribution of the displacements and stresses. Khoshgoftar *et al.* (2009) investigated thermo elastic analysis of a FGP cylinder under pressure. They assumed that all mechanical and electrical properties except Poisson ratio vary continuously along the thickness direction with a power function. Arefi and rahimi (2011, 2012) published some useful analyses about different structures made of functionally graded piezoelectric materials.

The present paper investigates the nonlinear response of a FGP annular plate that can be used as a

sensor or actuator in industrial application and micro positioning. For example, a FGP annular plate can be used in environment with very high pressure. Furthermore, this structure can be used as an actuator in micro positioning and medical application. A nonlinear analysis improves the responses of a structure especially for measurement instruments and very precision applications. These instruments because of application at serious and critical environment must be analyzed exactly. Hence, the present paper proposes an accurate and justifiable method for nonlinear analysis of an annular structure made of functionally graded piezoelectric materials (FGPM's).

2. Formulation

The nonlinear equations of a pressurized FG annular plate with two smart layers are introduced in the present section (Fig. 1). Classic Plate Theory (CPT) is employed for simulation of the displacements. The circular plate is assumed to be symmetric and therefore circumferential component of displacement must be zero. Based on CPT, the radial displacement of the plate can be decomposed into the displacement of mid plane and rotation about the mid plane (Allahverdizadeh *et al.* 2008, Ebrahimi and Rastgo 2008, Ugural 1981). Therefore, two nonzero components of displacement are

$$\begin{cases} u(r, z) = u_0(r) - z \frac{\partial w_0(r)}{\partial r} \\ w(r, z) = w_0(r) \end{cases} \quad (1)$$

where, u_0, w_0 are displacement components of the plate midplane ($z = 0$). In Fig. 1 (r, z) are radial and transverse components of employed coordinate system. a, b are inner and outer radii, $2h_e$ and $2h_p$ are thickness of FG and FGP layers, respectively.

The nonlinear components of strains can be obtained using (Lai 1999)

$$\{\varepsilon\} = 1/2 \{ \nabla \vec{u} + \nabla^T \vec{u} + (\nabla^T \vec{u})(\nabla \vec{u}) \} \quad (2)$$

where, $\vec{u} = (u, 0, w)$ is the vector of displacement. Due to symmetric distribution of loading, material properties and boundary conditions, the problem must be regarded as a symmetric problem and then $\varepsilon_{r\theta}$ and consequently $\sigma_{r\theta}$ must be zero. The nonlinear components of strains can be obtained using Eqs. (1) and (2) as follows (Allahverdizadeh *et al.* 2008)

$$\varepsilon_{rr} = \frac{\partial u_0}{\partial r} - z \frac{\partial^2 w_0}{\partial r^2} + 1/2 \left(\frac{\partial w_0}{\partial r} \right)^2, \varepsilon_{\theta\theta} = \frac{u_0}{r} - \frac{z}{r} \frac{\partial w_0}{\partial r}, \varepsilon_{r\theta} = 0 \quad (3)$$

The plate is composed of the piezoelectric materials. Therefore, the piezoelectric effect must be regarded in constitutive equation. The constitutive equation for piezoelectric materials is (Khoshgoftar *et al.* 2009, Qian *et al.* 2008)

$$\sigma_{ij} = C_{ijkl} \varepsilon_{kl} - e_{ijk} E_k \quad (4)$$

where, $\sigma_{ij}, \varepsilon_{kl}, E_k$ are the components of stress, strain and electric field, respectively. C_{ijkl}, e_{ijk} are the stiffness and piezoelectric coefficient, respectively. C_{ijkl}, e_{ijk} are the components of tensor with order 4 and 3 and in the general state have 81 and 27 components, respectively. Electric field E_k can be obtained

using a potential function $\phi(r, z)$ as follows (Khoshgoftar *et al.* 2009, Ebrahimi and Rastgo 2008)

$$\phi = \phi(r, z) \rightarrow \begin{cases} E_r = -\frac{\partial \phi(r, z)}{\partial r} \\ E_\theta = 0 \\ E_z = -\frac{\partial \phi(r, z)}{\partial z} \end{cases} \quad (5)$$

Due to symmetric distribution of the electric potential, the circumferential component of electric field E_θ is zero. The electric displacement, D_i in the electromechanical systems is the linear composition of the strain and electric field as follows (Khoshgoftar *et al.* 2009, Qian *et al.* 2008)

$$D_i = e_{ijk} \varepsilon_{jk} + \eta_{ik} E_k \quad (6)$$

where, η_{ik} are the dielectric coefficient. η_{ik} are the components of tensor with order 2 and in the general state have 9 components.

Due to small value of the plate thickness with respect to radius of the plate, the normal stress σ_{zz} and shear stresses σ_{xz} , σ_{yz} are neglected. The constitutive equations based on the plane stress condition for elastic solid section of the plate (FG) $-h_e \leq z \leq h_e$ are

$$\begin{cases} \sigma_{rr} = C^e_{rrr} \varepsilon_{rr} + C^e_{r\theta\theta} \varepsilon_{\theta\theta} \\ \sigma_{\theta\theta} = C^e_{\theta\theta r} \varepsilon_{rr} + C^e_{\theta\theta\theta} \varepsilon_{\theta\theta} \end{cases} \quad (7)$$

where, C^e_{ijkl} are stiffness coefficients for elastic solid section of the plate. The constitutive equations for piezoelectric sections of the plate (FGP) $h_e \leq |z| \leq h_e + h_p$ are

$$\begin{cases} \sigma_{rr} = C^p_{rrrr} \varepsilon_{rr} + C^p_{rr\theta\theta} \varepsilon_{\theta\theta} - e_{rrr} E_r - e_{rrz} E_z \\ \sigma_{\theta\theta} = C^p_{\theta\theta r} \varepsilon_{rr} + C^p_{\theta\theta\theta} \varepsilon_{\theta\theta} - e_{\theta\theta r} E_r - e_{\theta\theta z} E_z \end{cases} \quad (8)$$

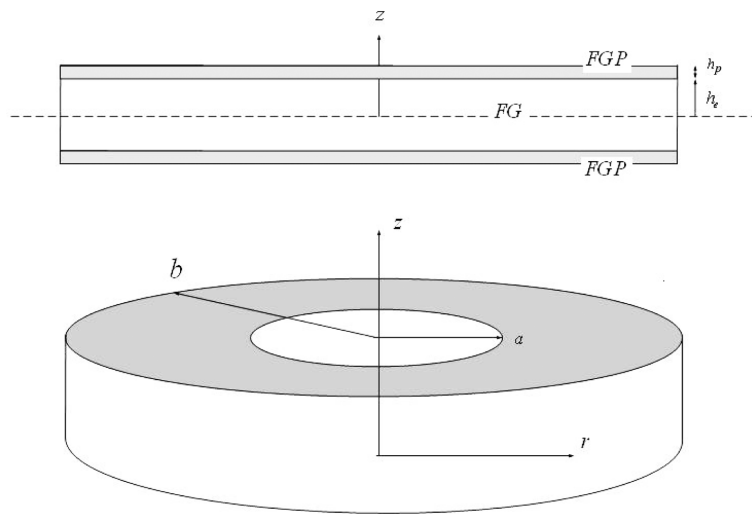


Fig. 1 The schematic figure of a FGP annular plate

The electric displacement equations for piezoelectric sections of the plate (FGP) $h_e \leq |z| \leq h_e + h_p$ are

$$\begin{cases} D_r = e_{rrr} \varepsilon_{rr} + e_{r\theta\theta} \varepsilon_{\theta\theta} + \eta_{rr} E_r + \eta_{rz} E_z \\ D_z = e_{zrr} \varepsilon_{rr} + e_{z\theta\theta} \varepsilon_{\theta\theta} + \eta_{zr} E_r + \eta_{zz} E_z \end{cases} \quad (9)$$

Using Eqs. (3), (5), (7), (8) and (9) the energy per unit volume of the plate \bar{u} can be analytically evaluated as follows (Arefi and rahimi 2012)

$$\bar{u} = \frac{1}{2} \{ \boldsymbol{\varepsilon}^T \boldsymbol{\sigma} - \mathbf{E}^T \mathbf{D} \} \rightarrow \bar{u} = \frac{1}{2} \{ \sigma_{rr} \varepsilon_{rr} + \sigma_{\theta\theta} \varepsilon_{\theta\theta} - D_r E_r - D_z E_z \} \quad (10)$$

Total energy equation of the plate must be evaluated with regarding the potential energy of the plate under pressure. The pressure can be assumed to be uniform or non uniform. The total energy of the plate is (GhannadPour and Alinia 2006, Alinia and GhannadPour 2009, Arefi and Rahimi 2010)

$$U = \iint_A \int_{-(h_e+h_p)}^{(h_e+h_p)} \bar{u}(r,z) dz dA - \int_A p(r) w dA \quad (11)$$

where, A defines the area of the plate. The energy equation can be divided for two different sections of the plate as follows

$$U = \iint_A \int_{-h_e}^{h_e} \frac{1}{2} \{ \sigma_{rr}^e \varepsilon_{rr} + \sigma_{\theta\theta}^e \varepsilon_{\theta\theta} \} dz dA + 2 \iint_A \int_{h_e}^{h_e+h_p} \frac{1}{2} \{ \sigma_{rr}^p \varepsilon_{rr} + \sigma_{\theta\theta}^p \varepsilon_{\theta\theta} - D_r E_r - D_z E_z \} dz dA - \int_A p(r) w dA \quad (12)$$

It is assumed that whole inner and outer edges of the plates are under fixed supports with no displacements and rotations. This means that the displacements and the slope of displacements must be vanished at inner and outer radii. Eq. (13) is considered such that satisfies mentioned boundary conditions. $f(z)$ in last function is considered to forced short circuited conditions between the top and bottom of piezoelectric section of the plates (Ebrahimi and Rastgo 2008, Allahverdizadeh *et al.* 2008). The procedure of solution can be continued with assumption of three fields for displacements and electric potential. The appropriate power function can be employed for these assumptions as follows (Ugural 1981)

$$\begin{aligned} u_0(r) &= [1 - (\frac{r}{a})^2]^2 \times [1 - (\frac{r}{b})^2]^2 \sum_{m=0} (U_m r^m) \\ w_0(r) &= [1 - (\frac{r}{a})^2]^2 \times [1 - (\frac{r}{b})^2]^2 \sum_{m=0} (W_m r^m) \\ \phi(r,z) &= f(z) [1 - (\frac{r}{a})^2]^2 \times [1 - (\frac{r}{b})^2]^2 \sum_{m=0} (\Phi_m r^m) \end{aligned} \quad (13)$$

As mentioned previously, $f(z)$ guaranties this assumption that electric potential at top and bottom of both piezoelectric layers must be zero. Therefore this function is (Ebrahimi and Rastgo 2008, Arefi and rahimi 2011)

$$\begin{aligned} \phi(z = h_e) &= \phi(z = h_e + h_p) = 0 \rightarrow \\ f(z) &= (1 - \{ \frac{2z - 2h_e - h_p}{h_p} \}^2) \end{aligned} \quad (14)$$

It can be found that three supposed functions for displacements and electric potential satisfies necessary (essential) boundary conditions related to imposed boundary conditions on the inner and outer edges. For example, the value of $u_0(r)$ at $r = a, b$ is zero identical to $\frac{\partial u_0(r)}{\partial r}$ at those edges.

Energy equation can be evaluated in terms of amplitude of the displacements U_m , W_m and the electric potential Φ_m as follows

$$U = U(U_m, W_m, \Phi_m) \quad (15)$$

The solution of the system can be obtained by minimizing the energy equation (Eq. (12)) with respect to characteristic value of the displacements and the electric potential (U_m , W_m , Φ_m) as follows

$$R_i = \frac{\partial U}{\partial q_i} = 0, q_i = U_m, W_m, \Phi_m \quad (16)$$

This minimizing tends to a system of algebraic nonlinear equations (Eq. (16)). The algebraic nonlinear equation can be solved and final solutions of the system may be analytically obtained.

3. Results and discussion

3.1 Material properties

Before solution of the problem, it is appropriate to define the material properties for FG and FGP layers, individually. For FG layer, it is assumed that the bottom of FG section of the plate is steel and top of that is ceramic. Therefore the distribution of the material properties for FG layer is (Dai *et al.* 2007)

$$E(z) = (E_c - E_m) \left(\frac{1}{2} + \frac{z}{2h_e} \right)^n + E_m \quad -h_e \leq z \leq h_e \quad (17)$$

where, $E(z = -h_e) = E_m$ and $E(z = h_e) = E_c$. “n” is non homogenous index that describes variation of different mechanical and electrical material properties along the thickness direction between a layer of full metal till a layer of full ceramic. “n=0” represent a material made of pure ceramic and $n \rightarrow \infty$ represent a material made of pure metal (except $z=h/2$ that is ceramic). The nonzero and finite values of “n” can be employed for medium composition of metal and ceramic or every two different materials. The distribution of the mechanical and electrical properties for FGP layers can be supposed as a power function along the thickness direction as follows (Allahverdizadeh 2008, Arefi and Rahimi 2010)

$$E(z) = E_i \left(\frac{|z|}{h_e} \right)^n \quad h_e \leq |z| \leq h_e + h_p \quad (18)$$

where, E_i is the value of every mechanical and electrical property at $|z| = h_e$. By these assumptions (Eqs. (17) and (18)) the energy equation can be obtained using Eq. (12). By minimization of the energy equation using Eqs. (15) and (16), the responses of the nonlinear analysis of the system can be analytically evaluated. The variable material properties of the FGP plate for two sections are selected as follows

$$\text{Elastic solid section : } C_{rrr}^e = C_{\theta\theta\theta}^e = \frac{E_1(z)}{1-\nu^2}, C_{rr\theta\theta}^e = C_{\theta\theta rr}^e = \frac{\nu E_1(z)}{1-\nu^2} \quad (19)$$

$$E_1(z) = (E_c - E_m) \left(\frac{1}{2} + \frac{z}{2h_e} \right)^n + E_m \quad -h_e \leq z \leq h_e$$

$$\text{Piezoelectric section : } C_{rrr}^p = C_{\theta\theta\theta}^p = \frac{E_2(z)}{1-\nu^2}, C_{rr\theta\theta}^p = C_{\theta\theta rr}^p = \frac{\nu E_2(z)}{1-\nu^2}$$

$$E_2(z) = E_{h_e} \left(\frac{|z|}{h_e} \right)^n \quad h_e \leq |z| \leq h_e + h_p$$

$$e_{rr} = e_1(z), e_{r\theta\theta} = e_{\theta\theta r} = e_{rz} = e_{zr} = e_{z\theta\theta} = e_{\theta\theta z} = e_2(z)$$

$$\eta_{rr} = \eta_{zz} = \eta_{1h_e}(z), \eta_{rz} = \eta_{zr} = \eta_{2h_e}(z)$$

$$e_1(z) = e_{1h_e} \left(\frac{|z|}{h_e} \right)^n, e_2(z) = e_{2h_e} \left(\frac{|z|}{h_e} \right)^n, \eta_{1h_e}(z) = \eta_{1h_e} \left(\frac{|z|}{h_e} \right)^n, \eta_{2h_e}(z) = \eta_{2h_e} \left(\frac{|z|}{h_e} \right)^n$$

$$\text{for } h_e \leq |z| \leq h_e + h_p$$

$$E_c = 3.8 \times 10^{11} \text{ Pa}, E_m = 2 \times 10^{11} \text{ Pa}, E_{h_e} = 7.6 \times 10^{10} \text{ Pa}$$

$$e_{1h_e} = 0.35 \text{ VmN}^{-1}, e_{2h_e} = -0.16 \text{ VmN}^{-1}, \eta_{1h_e} = 9.03 \times 10^{-11} \text{ mN}^{-1}, \eta_{2h_e} = 5.62 \times 10^{-11} \text{ mN}^{-1}$$

$$a = 0.03 \text{ m}, b = 0.15 \text{ m}, h_e = 0.003 \text{ m}, h_p = e \times h_e$$

3.2 Evaluation of the results

In the present section, most important results of this analysis are considered. After evaluation of the unknown amplitudes U_m , W_m , Φ_m the distribution of both displacements and electric potential can be obtained using Eq. (13). The distribution of the stress and strain may be analytically evaluated using Eqs. (3), (7) and (8).

Fig. 2 shows the distribution of the stiffness coefficient along the wall of the cylinder for different values of the non homogenous index (n).

Fig. 3 shows the distribution of the characteristic value of the transverse displacement (W_m) in terms of the normal applied pressure. This figure presents the nonlinearity nature of the problem, exactly. For example, with increasing the pressure from 100 to 500 MPa, the maximum transverse displacement increases 3.01 times of it's initial value.

Fig. 4 shows the distribution of the characteristic value of the electric potential (Φ_m) in terms of the normal applied pressure. This figure verifies the nature of nonlinearity of the problem similar to Fig. 3.

Procedure of the numerical solution indicates that with increasing the non homogenous index, the trend of displacements, potential, stresses and other components depend on the ratio of the piezoelectric thickness respect to solid elastic thickness $e = h_p/h_e$. Because of power distribution of the properties along the thickness direction for piezoelectric layer based on Eq. (18), the bending stiffness of the plate increases with increasing the non homogenous index (n). Therefore with increasing the non homogenous index, the convergence of electrical and mechanical components to an asymptotic value depends on the ratio $e = h_p/h_e$. For small value of $e = h_p/h_e$, the mechanical and electrical components converge rapidly for $n \geq 10$.

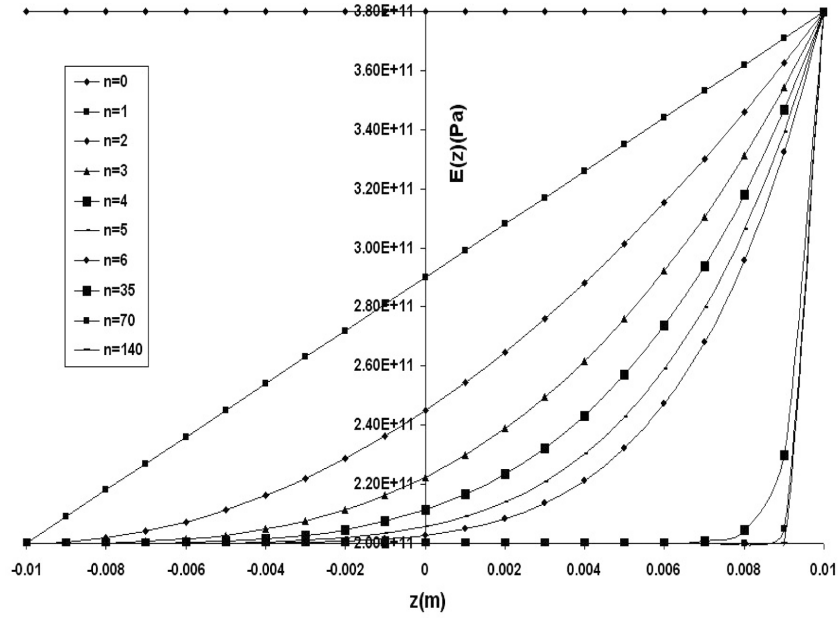


Fig. 2 Distribution of the stiffness coefficient along the thickness direction for different values of the non homogenous index

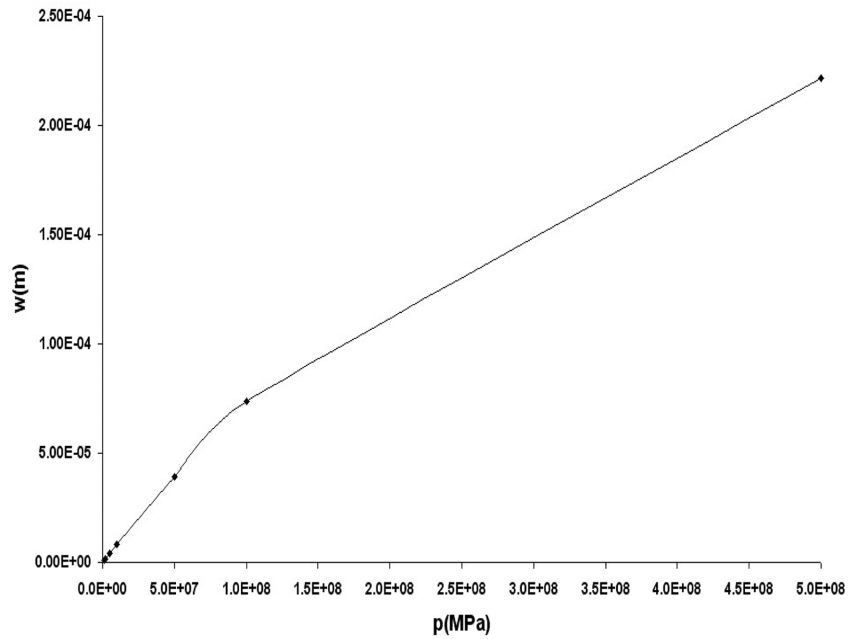


Fig. 3 The nonlinear distribution of the characteristic value of the transverse displacement (W_m) in terms of the applied pressure

Fig. 5 shows the distribution of the characteristic value of the transverse displacement (W_m) in terms of the non homogenous index (n).

Fig. 6 shows the distribution of the characteristic value of the radial displacement (U_m) in terms of

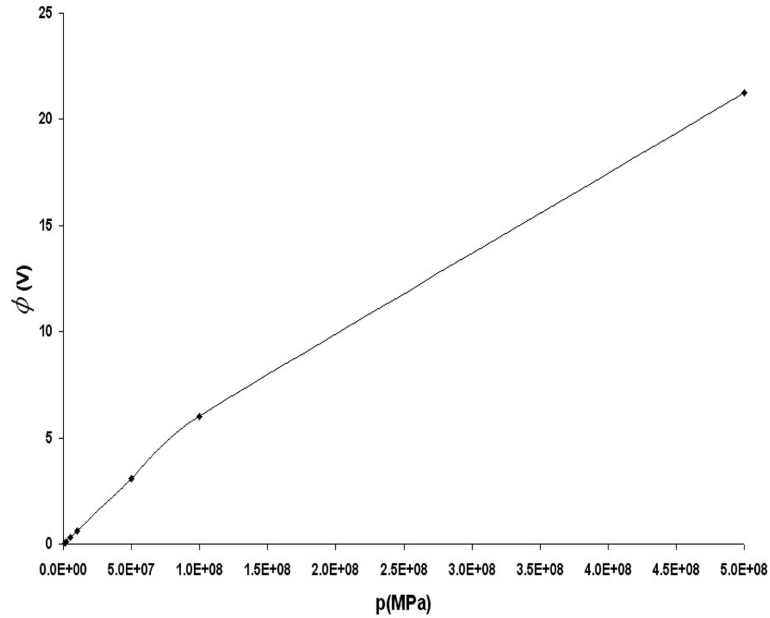


Fig. 4 The nonlinear distribution of the characteristic value of the electric potential (Φ_m) in terms of the applied pressure

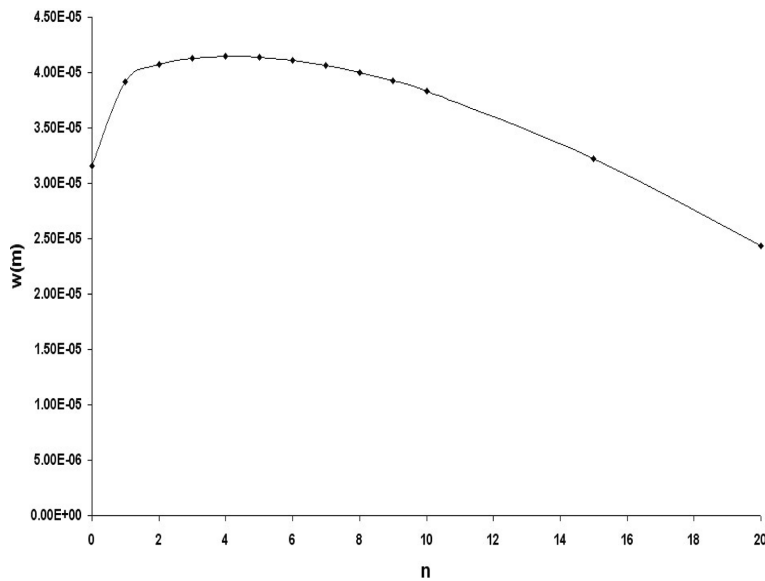


Fig. 5 Distribution of the characteristic value of the transverse displacement (W_m) in terms of the non homogenous index (n) for $e = \frac{h_p}{h_e} = \frac{1}{6}$

the non homogenous index (n). This figure is similar to Fig. 5 and with increasing the value of the non homogenous index don't converge to an asymptotic value.

Fig. 7 shows the distribution of the characteristic value of the electric potential (Φ_m) in terms of the non homogenous index (n). This figure is similar to Figs. 5 and 6 and with increasing the value

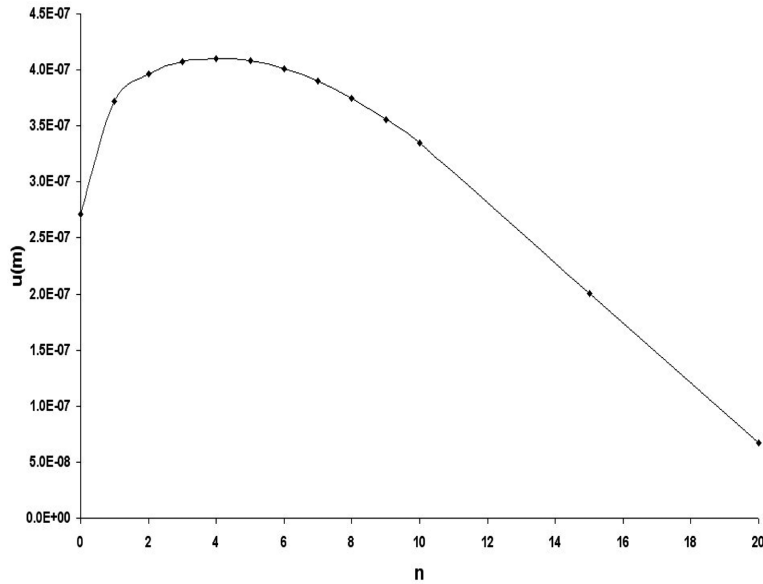


Fig. 6 Distribution of the characteristic value of the radial displacement (U_m) in terms of the non homogenous index (n) for $e = \frac{h_p}{h_e} = \frac{1}{6}$

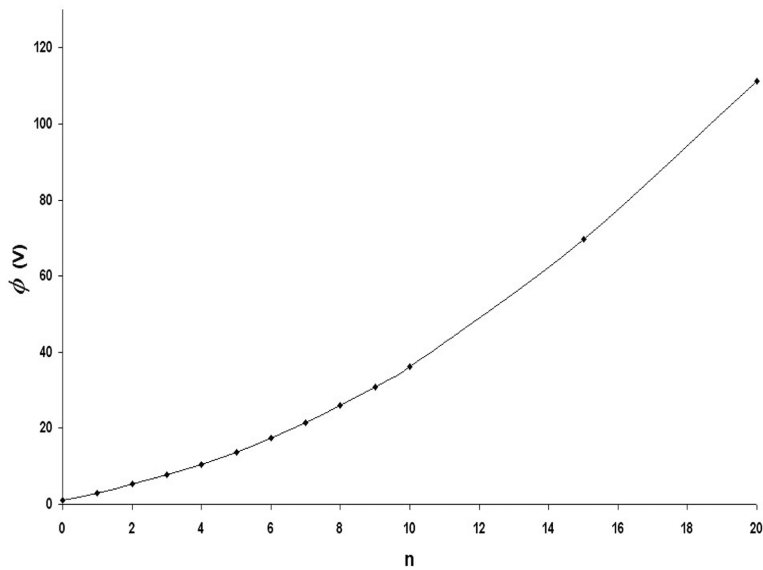


Fig. 7 Distribution of the characteristic value of the electric potential (Φ_m) in terms of the non homogenous index (n) for $e = \frac{h_p}{h_e} = \frac{1}{6}$

of the non homogenous index don't converge to an asymptotic value.

Figs. 8 and 9 show the radial distribution of the transverse displacement and the radial displacement for five values of the non homogenous index. Figs. 10 and 11 show the radial distribution of the radial and circumferential stresses for five values of the non homogenous index.

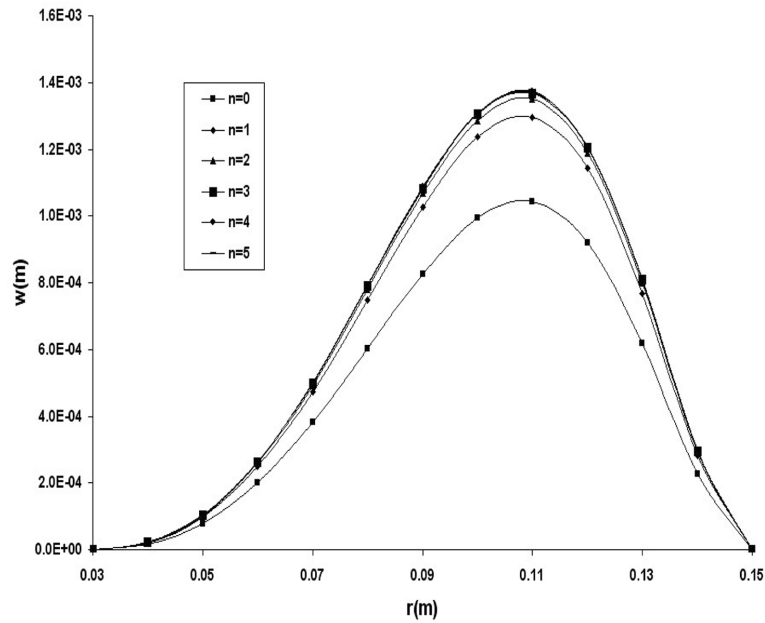


Fig. 8 The radial distribution of the transverse displacement for five values of the non homogenous index (n)

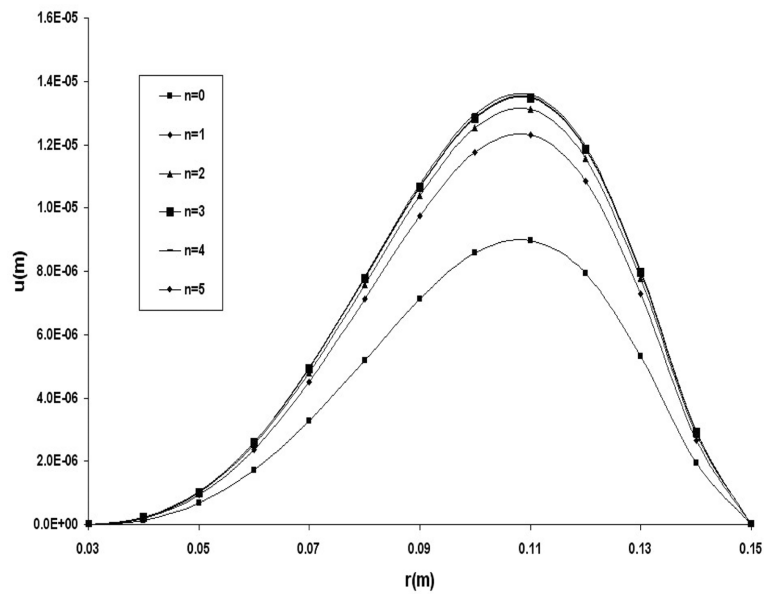


Fig. 9 The radial distribution of the radial displacement for five values of the non homogenous index (n)

3.2.1 Linear analysis, comparison with nonlinear responses

For investigation of the effect of the geometric nonlinearity on the response of the system, this section evaluates the linear response of the system. A comprehensive comparison can be performed to analyze the effect of the geometric nonlinearity on the responses.

Figs. 12 and 13 show the distribution of the transverse displacement and the electric potential for

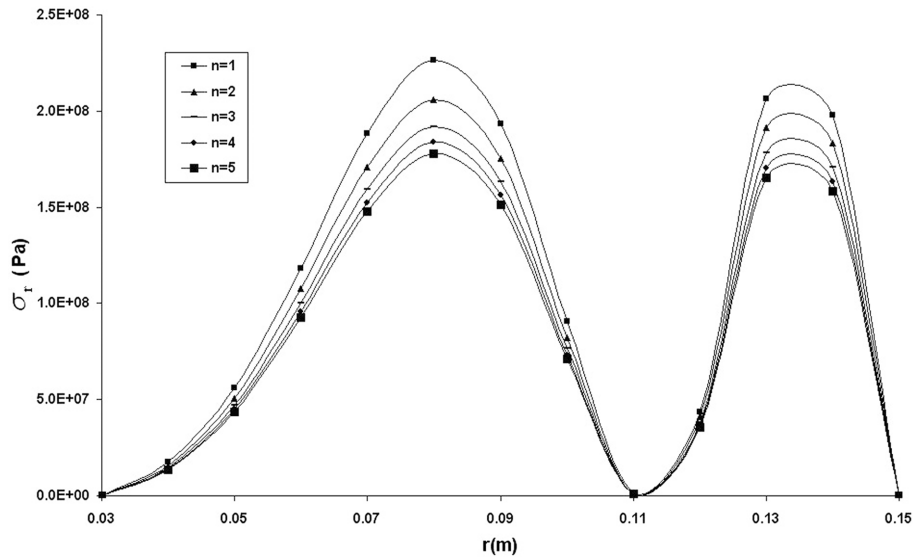


Fig. 10 The radial distribution of the radial stress for five values of the non homogenous index (n)

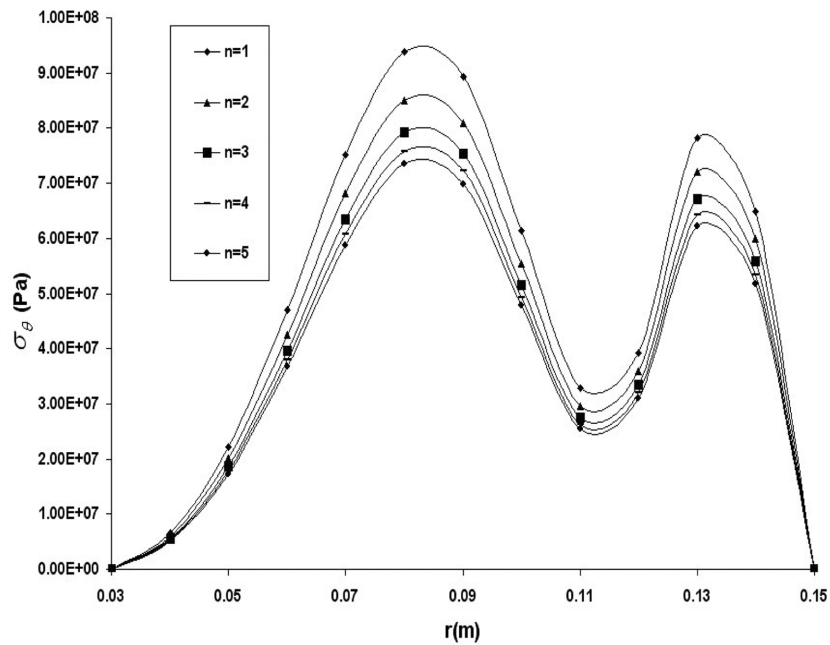


Fig. 11 The distribution of the circumferential stress for five values of the non homogenous index (n)

different values of the non homogenous index (n) based on the linear and nonlinear analyses.

3.2.2 Investigation of the effect of piezoelectric thickness on the convergence of the responses

In the previous section, it is investigated the distribution of the displacements and the electric potential in terms of various values of the non homogenous index. Figs. 5, 6 and 7 have shown the

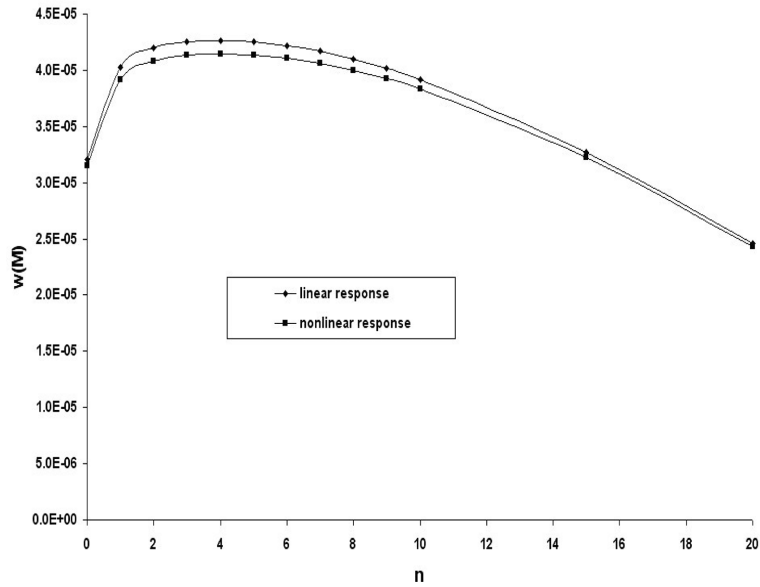


Fig. 12 Comparison between the nonlinear and linear responses (maximum transverse displacement)

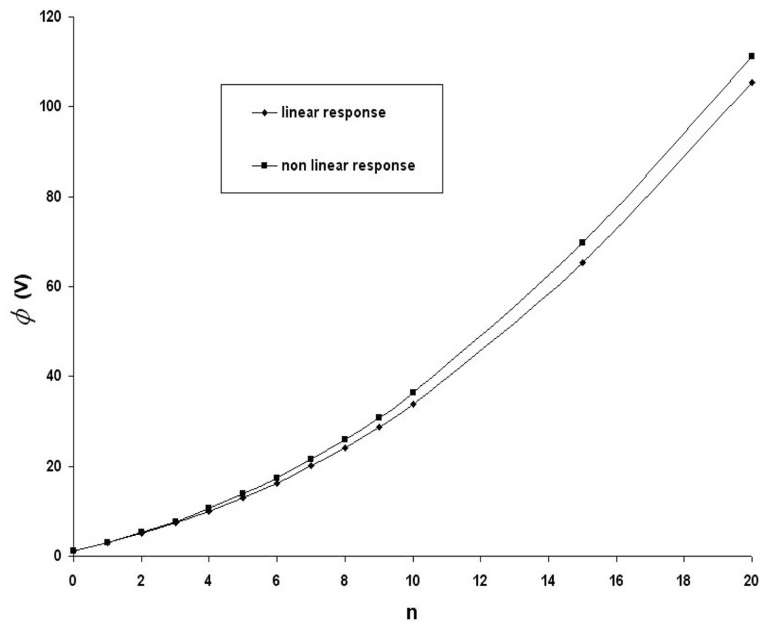


Fig. 13 Comparison between the nonlinear and linear responses (characteristic value of the electric potential (Φ_m))

distribution of the mechanical and electrical components in terms of different values of the non homogenous index. Because of considerable value of the ratio of the piezoelectric thickness with respect to solid elastic thickness, these figures don't converge in any way. With decreasing the value of the piezoelectric thickness with respect to solid elastic thickness, the values of the radial and the

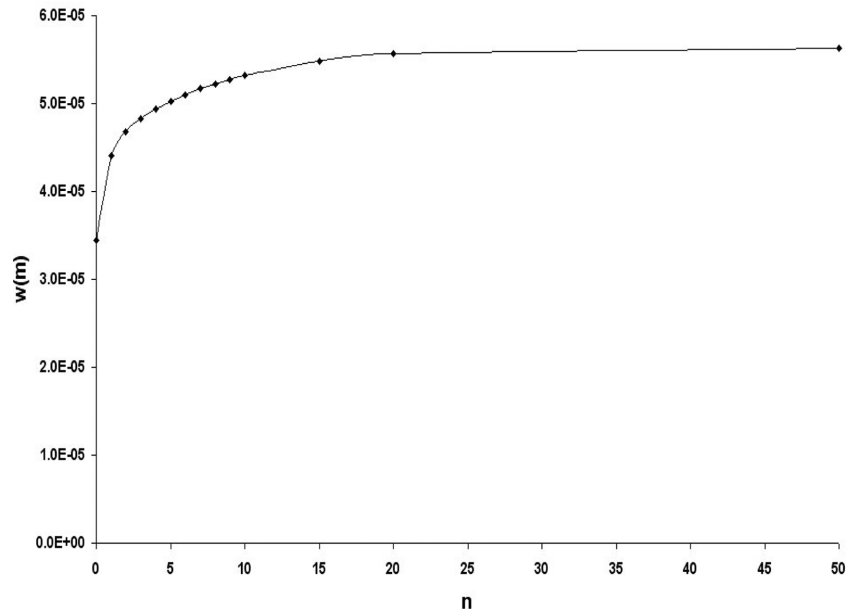


Fig. 14 Distribution of the characteristic value of the transverse displacement (W_m) in terms of the non homogenous index for $e = \frac{h_p}{h_e} = \frac{1}{30}$

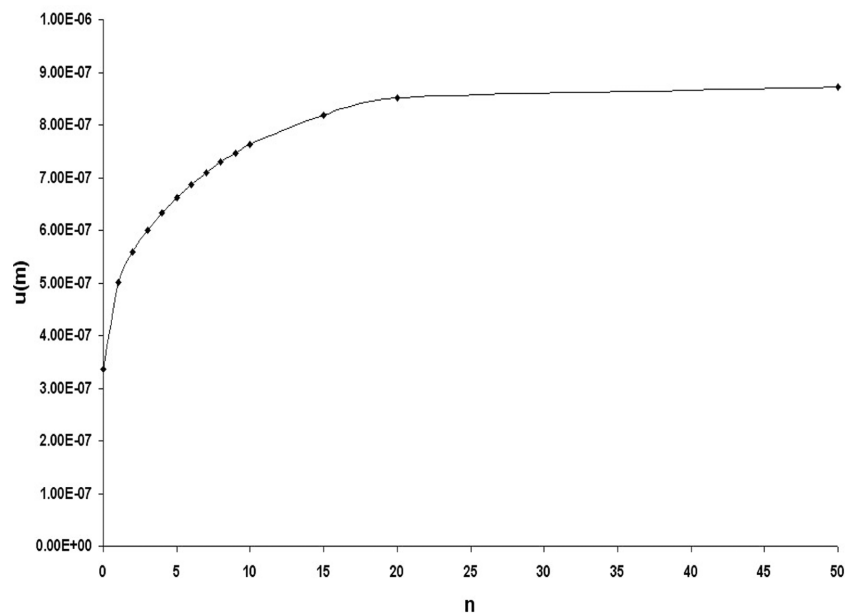


Fig. 15 Distribution of the characteristic value of the radial displacement (U_m) in terms of the non homogenous index for $e = \frac{h_p}{h_e} = \frac{1}{30}$

transverse displacement converge rapidly. Figs. 14 and 15 shows the distribution of the transverse and radial displacements in terms of the non homogenous index for $e = \frac{1}{30}$.

4. Conclusions

1. Measurement instruments and tools are very applicable structures that have technical usage such as at chemical processes, nuclear reactors and weapon productions. Application of these instruments in critical and important instances justifies the necessity of a nonlinear analysis about them. A nonlinear analysis can offer an accurate and justifiable tool for analysis of these structures.
2. Convergence of mechanical and electrical components such as displacements, stresses and electric potential considerably depend on the ratio of the piezoelectric thickness with respect to solid elastic thickness (e). For small value of e , mechanical and electrical components converge clearly for the non homogenous index greater than 10.
3. The radial stress of mid-plane of the plate becomes zero for three values of the radial position. Figs. 10 and 11 indicates that the location of the maximum and minimum values of the radial and circumferential stresses don't depend on the non homogenous index. The maximum and minimum values of the radial and circumferential stresses depend on the non homogenous index.
4. A linear analysis is performed and the obtained results are compared with those results that are extracted from nonlinear analysis. This comparison indicates that the effect of the geometric nonlinearity must be regarded in the analysis of FGP structures especially for measurement instruments such as sensor.

References

- Allahverdzadeh, A., Naei, M.H. and Nikkhah B.M. (2008a), "Vibration amplitude and thermal effects on the nonlinear behavior of thin circular functionally graded plates", *Compos. Struct.*, **50**(3), 445-454.
- Allahverdzadeh, A., Naei, M.H. and Nikkhah, B.M. (2008b), "Nonlinear free and forced vibration analysis of thin circular functionally graded plates", *J. Sound. Vib.*, **310**(4-5), 966-984.
- Alinia, M.M. and Ghannadpour, S.A.M. (2009), "Nonlinear analysis of pressure loaded FGM plates", *Compos. Struct.*, **88**(3), 354-359.
- Arefi, M. and Rahimi, G.H. (2010), "Thermo elastic analysis of a functionally graded cylinder under internal pressure using first order shear deformation theory", *Sci. Res. Essays.*, **5**(12), 1442-1454.
- Arefi, M., Rahimi, G.H. and Khoshgoftar, M.J. (2011), "Optimized design of a cylinder under mechanical, magnetic and thermal loads as a sensor or actuator using a functionally graded piezomagnetic material", *Int. J. Phys. Sci.*, **6**(27), 6315-6322.
- Rahimi, G.H. Arefi, M. and Khoshgoftar, M.J. (2011), "Application and analysis of a functionally graded piezoelectrical rotating cylinder as a mechanical sensor subjected to pressure and thermal loads", *Appl. Math. Mech - Eng.*, **32**(9), 997-1008.
- Arefi, M. and Rahimi, G.H. (2011), "Non linear analysis of a functionally graded square plate with two smart layers as sensor and actuator under normal pressure", *Smart. Struct. Syst.*, **8**(5), 433-448.
- Arefi, M. and Rahimi, G.H. (2012), "Three dimensional multi field equations of a functionally graded piezoelectric thick shell with variable thickness, curvature and arbitrary nonhomogeneity", *Acta Mech.*, **223**, 63-79.
- Arefi, M. and Rahimi, G.H. (2011), "General formulation for the thermoelastic analysis of an arbitrary structure made of functionally graded piezoelectric materials based on the energy method", *Mech. Eng.*, **62**(4), 221-236.
- Boresi, A. (1993), *Advanced mechanics of materials*, 5th Ed., John wiley & Sons press.
- Chen, W.Q. Lu, Y. Ye, J.R. and Cai, J.B. (2002), "3D electroelastic fields in a functionally graded piezoceramic hollow sphere under mechanical and electric loading", *Arch. Appl. Mech.*, **72**, 39-51.
- Chen, Y. and Shi, Z.F. (2005), "Analysis of a functionally graded piezothermoelastic hollow cylinder", *J. Zhej. Univ. Sci.*, **6A**(9), 956-961.
- Chih, P.W. and Yun, S.S. (2007), "Exact solution of functionally graded piezoelectric shells under cylindrical bending", *Int. J. Solids. Struct.*, **44**(20), 6450-6472.

- Dai, H.L. Fu, Y.M. and Yang, J.H. (2007), "Electromagnetoelastic behaviors of functionally graded piezoelectric solid cylinder and sphere", *Acta Mech. Sinica.*, **23**(1), 55-63.
- Ebrahimi, F. and Rastgo, A. (2008), "An analytical study on the free vibration of smart circular thin FGM plate based on classical plate theory", *Thin. Wall. Struct.*, **46**(12), 1402-1408.
- GhannadPour, S.A.M. and Alinia, M.M. (2006), "Large deflection behavior of functionally graded plates under pressure loads", *Compos. Struct.*, **75**(1-4), 67-71.
- HuiShen, S. (2007), "Nonlinear thermal bending response of FGM plates due to heat conduction", *Compos. Part. B - Eng.*, **38**(2), 201-215.
- Khoshgoftar, M.J. Ghorbanpour Arani, A. and Arefi, M. (2009), "Thermoelastic analysis of a thick walled cylinder made of functionally graded piezoelectric material", *Smart. Mater. Struct.*, **18**(11).
- Lai, M., Rubin, D. and Krempl, E. (1999), *Introduction to continuum mechanics*, 3rd Ed., Butterworth-Heinemann press.
- Lu, P. Lee, H.P. and Lu, C. (2005), "An exact solution for functionally graded piezoelectric laminated in cylindrical bending", *Int. J. Mech. Sci.*, **47**, 437-458.
- Ma, L.S. and Wang, T.J. (2004), "Relationships between axisymmetric bending and buckling solutions of FGM circular plates based on third-order plate theory and classical plate theory", *Int. J. Solids. Struct.*, **41**(1), 85-101.
- Malekzadeh, P. and Vosoughi, A.R. (2009), "DQM large amplitude vibration of composite beams on nonlinear elastic foundations with restrained edges", *Commun. Nonlin. Sci. Num. Sim.*, **14**(3), 906-915.
- Ootao, Y. and Tanigawa, Y. (2007), "Transient piezothermoelastic analysis for a functionally graded thermopiezoelectric hollow sphere", *Compos. Struct.*, **81**(4), 540-549.
- Qian, Z.H. Jin, Feng. Lu, T. and Kishimoto, Kikuo. (2008), "Transverse surface waves in functionally graded piezoelectric materials with exponential variation", *Smart. Mater. Struct.*, **17**(6).
- Sarfaraz KhabbSaz, R., Dehghan Manshadi, B. and Abedian, A. (2009), "Non-linear analysis of FGM plates under pressure loads using the higher-order shear deformation theories", *Compos. Struct.*, **89**, 333-344
- Shi, Z.F. and Chen, Y. (2004), "Functionally graded piezoelectric cantilever beam under load", *Arch. Appl. Mech.*, **74**(3-4), 237-247.
- Soufyane, A. (2009), "Exponential stability of the linearized non uniform Timoshenko beam", *Nonlinear Anal - Real.*, **10**, 1016-1020.
- Ugural, A.C. (1981), *Stress in plate and shells*, McGraw-Hill.
- Woo, J. and Meguid, S.A. (2001), "Nonlinear analysis of functionally graded plates and shallow shells", *Int. J. Solids. Struct.*, **38**(42-43), 7409-7421.

Nomenclature

C_{ijkl}	: stiffness coefficient
C_{ijkl}^e	: stiffness coefficient for FG layer
C_{ijkl}^p	: stiffness coefficient for FGP layer
D_i	: electric displacement
e_{ijk}	: piezoelectric coefficient
E_k	: electric field components
$2h_e$: thickness of FG layer
h_p	: thickness of FGP layers
a, b	: Inner and outer radii
p	: applied pressure
x, y, z	: components of coordinate system
u, v, w	: displacement components at a general point
u_0, v_0, w_0	: displacement components at mid-plane
ε_{ij}	: strain components
σ_{ij}	: stress components
\bar{u}	: energy per unit volume
U	: total energy of system
η_{ik}	: dielectric coefficient
U_m, W_m, Φ_m	: amplitude of assumed function
ϕ	: electric potential